Differential Behaviors of Atrial Versus Ventricular Fibroblasts

A Potential Role for Platelet-Derived Growth Factor in Atrial-Ventricular Remodeling Differences

Brett Burstein, BSc; Eric Libby, BSc; Angelino Calderone, PhD; Stanley Nattel, MD

Background—In various heart disease paradigms, atria show stronger fibrotic responses than ventricles. The possibility that atrial and ventricular fibroblasts respond differentially to pathological stimuli has not been examined.

Methods and Results—We compared various morphological, secretory, and proliferative response indexes of canine atrial versus ventricular fibroblasts. Cultured atrial fibroblasts showed faster cell surface area increases, distinct morphology at confluence, and greater α-smooth muscle actin expression than ventricular fibroblasts. Atrial fibroblast proliferation ([^{3}H]thymidine incorporation) responses were consistently greater for a range of growth factors, including fetal bovine serum, platelet-derived growth factor (PDGF), basic fibroblast growth factor, angiotensin II, endothelin-1, and transforming growth factor-β_1. Normal atrial tissue showed larger myofibroblast density compared with ventricular tissue, and the difference was exaggerated by congestive heart failure. Congestive heart failure atria showed larger fractions of fibroblasts in mitotic phases compared with ventricles and displayed enhanced gene expression of fibroblast-selective markers (collagen-1, collagen-3, fibronectin-1). Gene microarrays revealed 225 differentially expressed transcript probe sets between paired atrial and ventricular fibroblast samples, including extracellular matrix (eg, fibronectin, laminin, fibulin), cell signaling (PDGF, PDGF receptor, angiopoietin, vascular endothelial growth factor), structure (keratin), and metabolism (xanthine dehydrogenase) genes, identifying PDGF as a candidate contributor to atrial-ventricular fibroblast differences. PDGF receptor gene expression was greater in normal atrium compared with ventricle, and congestive heart failure differentially enhanced atrial versus ventricular PDGF and PDGF receptor gene expression. PDGF receptor protein expression and α-smooth muscle actin protein expression were enhanced in isolated congestive heart failure fibroblasts. The PDGF receptor tyrosine kinase inhibitor AG1295 eliminated fetal bovine serum– and transforming growth factor-β_1–stimulated atrial-ventricular fibroblast proliferative response differences.

Conclusions—Atrial fibroblasts behave differently than ventricular fibroblasts over a range of in vitro and in vivo paradigms, with atrial fibroblasts showing enhanced reactivity that may explain greater atrial fibrotic responses. PDGF signaling is particularly important for atrium-selective fibroblast responses and may represent a novel target for arrhythmogenic atrial structural remodeling prevention. (***Circulation*. 2008;117:1630-1641.**)

Key Words: atrial fibrillation ■ extracellular matrix ■ fibrosis ■ heart failure ■ remodeling

Cardiac fibroblasts secrete extracellular matrix proteins that produce cardiac remodeling[1] and have become a focus of therapeutic intervention, particularly for congestive heart failure (CHF). Traditional ion channel–targeting antiarrhythmic approaches have proved inadequate for atrial fibrillation (AF), and interest is increasing in atrial remodeling as a potential therapeutic AF target.[2,3] In experimental CHF, atrial fibrosis and associated conduction impairments provide a substrate for sustained AF.[4] Atrial fibrosis greatly exceeds ventricular fibrosis (≈20-fold greater) in this model.[5] Mice with cardiac-specific overexpression of the profibrotic factors transforming growth factor-β_1 (TGFβ_1)[6,7] and angiotensin-converting enzyme[8] show atrial fibrosis, conduction abnormalities, and AF with unchanged ventricular size, function, and structure. We hypothesized that differences between atrial and ventricular fibroblast responsiveness might contribute to atrium-selective fibrotic behaviors. To address this hypothesis, we studied in parallel the proliferative responses

Received April 26, 2007; accepted February 5, 2008.

From the Departments of Medicine (B.B., S.N.) and Physiology (A.C.), Montreal Heart Institute and Université de Montréal, and Departments of Pharmacology and Therapeutics (B.B., S.N.) and Physiology (E.L.), McGill University, Montreal, Quebec, Canada.

The online-only Data Supplement, which consists of Methods, tables, and figures, can be found with this article at http://circ.ahajournals.org/cgi/content/full/CIRCULATIONAHA.107.748053/DC1.

Correspondence to Stanley Nattel, 5000 Belanger St E, Montreal, H1T 1C8, Quebec, Canada. E-mail stanley.nattel@icm-mhi.org

Circulation **is available at http://circ.ahajournals.org** **DOI: 10.1161/CIRCULATIONAHA.107.748053**

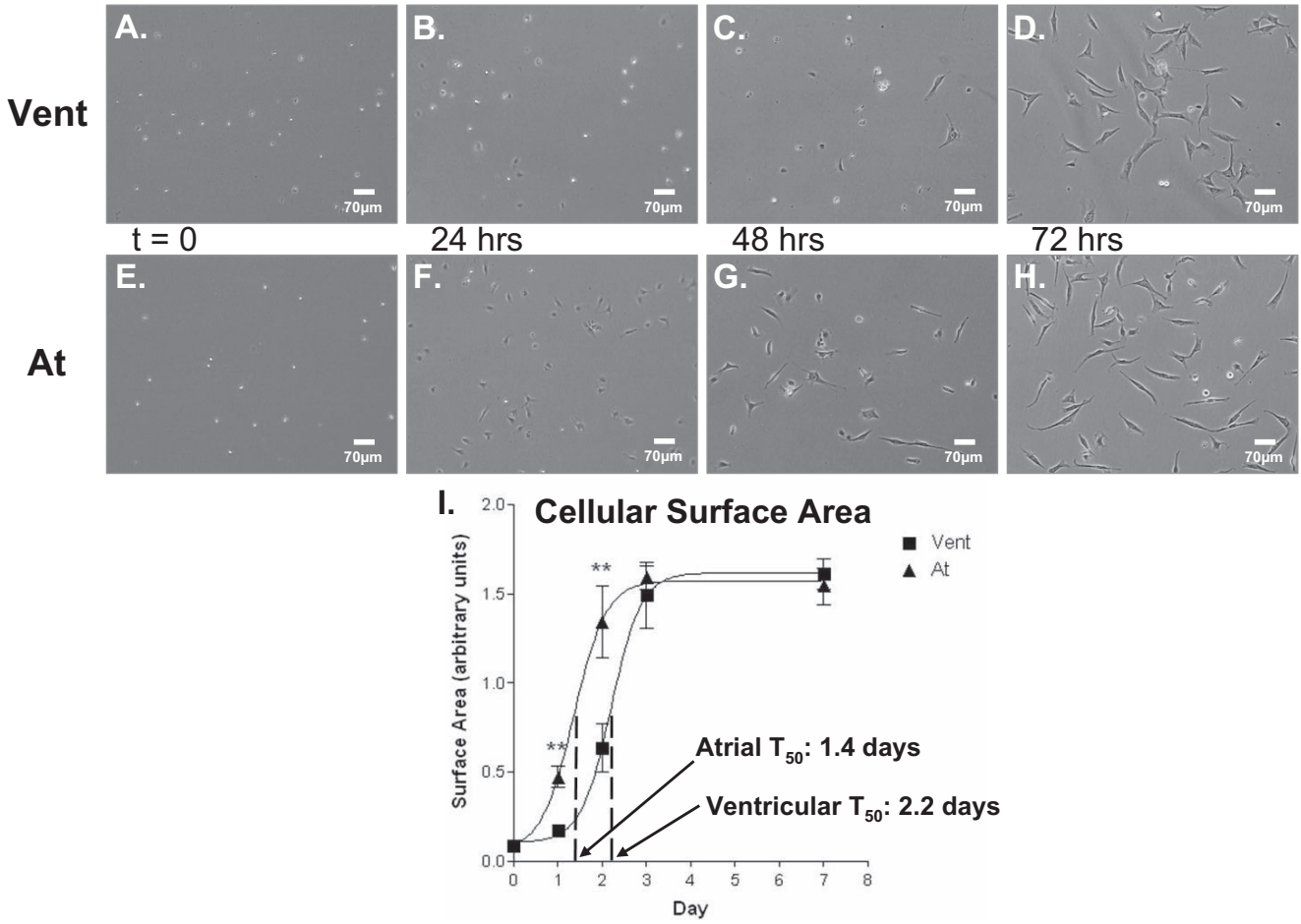

Figure 1. Bright-field images of primary-passage ventricular (Vent; A through D) and atrial (At; E through H) fibroblasts (magnification ×10; bar=70 μm). I, Mean±SEM cellular surface area. T_{50} is half-maximal growth-time. n=6 pairs. $^{**}P<0.01$, atrial vs ventricular values on the same day.

of atrial and ventricular fibroblasts isolated from individual canine hearts, assessed their gene expression profiles, and evaluated their response to platelet-derived growth factor (PDGF) receptor (PDGFR) stimulation and inhibition. We subsequently sought evidence for corresponding differences in vivo.

Clinical Perspective p 1641

Methods

This section summarizes key methods in abbreviated form. A detailed description of all methods is found in the Methods section of the online-only Data Supplement.

Cell Isolation, Culture, and Characterization

Experiments were performed with cardiac fibroblasts isolated, cultured, and characterized as described previously[9] from normal adult male 23- to 31-kg mongrel dogs (n=22). Preliminary studies revealed similar behavior in left atrial appendage– and left atrial free wall–derived fibroblasts (online-only Data Supplement Figure I). For practical purposes (tissue availability), further in vitro experiments used only first-passage cells from the left atrial appendage and left ventricular free wall. First-passage cells demonstrated >95% coexpression of α-smooth muscle actin (αSMA) and vimentin (online-only Data Supplement Figure II), indicating a myofibroblast phenotype resembling the activated cell type involved in remodeling and fibrosis. In all experiments, paired atrial and ventricular cell samples from each dog were plated in parallel at equal density, allowed to adhere for 24 hours, and then rendered quiescent in serum-free medium for 24 hours before treatment.

Morphological Analysis

Bright-field images of primary-passage atrial and ventricular fibroblasts (n=6 pairs per time point) were obtained after isolation (t=0) and at culture days 1, 2, 3, and 7 (at confluence). Duplicate random-field images were taken each day, coded, and quantified by an observer blinded to cell type. Cells were measured along their 2 longest perpendicular axes. The product of the long and short axes provided an index of surface area and the ratio of long to short axis, an index of cell morphology. Half-maximal growth times were quantified by nonlinear sigmoidal function regression.

Western Blot Analysis

First-passage atrial and ventricular fibroblasts (n=6 dogs per observation) in the exponential growth phase were plated at 150 cells per 1 mm^2. Proteins were extracted, quantified, and processed as previously described.[9] Protein samples (10 μg per lane) were separated with 10% PAGE-SDS electrophoresis and then transferred to polyvinylidene difluoride membranes. Membranes were blocked and incubated with mouse anti-αSMA (1/20 000), rabbit anti-PDGFRα (1/1000), and mouse anti-GAPDH (1/5000) primary antibodies, followed by either anti-mouse (1/10 000) or anti-rabbit (1/10 000) horseradish peroxidase–conjugated secondary antibodies. Signals were detected with chemiluminescence and quantified by video densitometry. Protein band intensities are expressed relative to GAPDH.

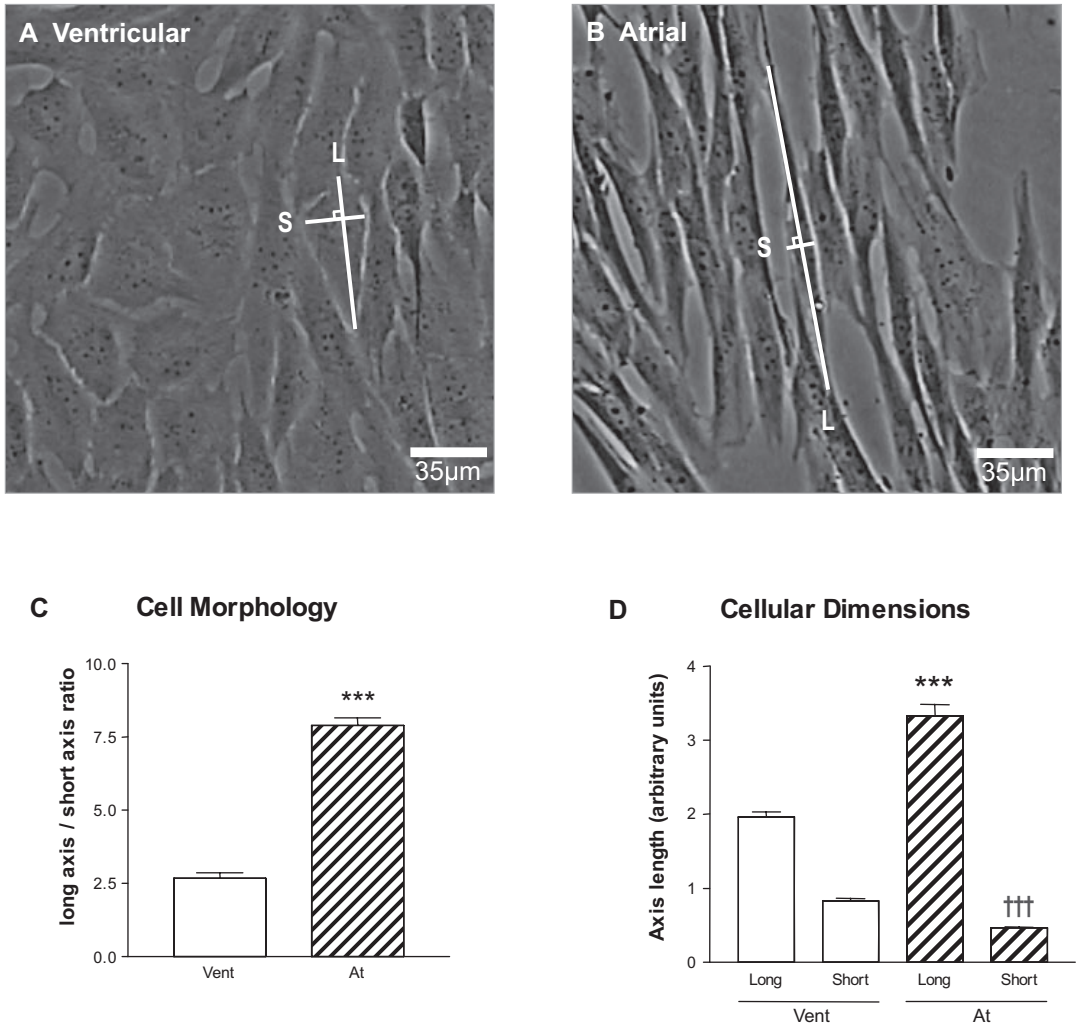

Figure 2. Bright-field images of primary-passage ventricular (Vent; A) and atrial (At; B) fibroblasts at confluence (magnification ×20; bar=35 μm). Long (L) and short (S) axes are indicated by perpendicular lines. C, Mean±SEM ratio of long axis to short axis. n=6 pairs. ***$P<0.001$. D, Cellular dimensions; mean±SEM; n=6 pairs. ***$P<0.001$ vs ventricular long axis; †††$P<0.001$ vs ventricular short axis.

[^{3}H]Thymidine Incorporation

Fibroblast proliferation was evaluated by [^{3}H]thymidine uptake.[9] Cells were plated at 50 cells per 1 mm^2 (n=6 to 11 per experiment) and after adhesion and quiescence were stimulated for 24 hours with 7% fetal bovine serum (FBS), PDGF-AB (10 ng/mL), basic fibroblast growth factor (5 ng/mL), angiotensin II (100 nmol/L), endothelin-1 (10 nmol/L), or TGFβ_1 (0.15 ng/mL). In 6 additional experiments, cells were treated for 24 hours with 7% FBS or TGFβ_1 in the presence of PDGFR tyrosine kinase inhibitor AG1295 (10 μmol/L) or vehicle. Data are expressed as fold change relative to baseline.

Canine DNA Microarrays

Total RNA was isolated from first-passage cells (n=5 per group) grown to confluence in 7% FBS.[10] After RNA quality control, 3-μg samples were fragmented and hybridized to Affymetrix Canine_2 microarrays. Chips were stained, washed, and visualized on an Affymetrix GeneChip Scanner 3000. Interarray brightness differences were corrected with Invariant Set Normalization in dChip. The model-based expression index integrating each gene probe intensity into a representative gene expression value was then computed.[11] Significance Analysis for Microarrays was applied to detect differentially expressed genes with q<5.

CHF and Sham Control Dogs

An additional 32 dogs (20 to 35 kg) received a right ventricular tachypacemaker,[4,5,11] which was either programmed for 2-week ventricular-tachypacing at 240-bpm to induce CHF (n=17) or left inactivated (control; n=15). Paired atrial and ventricular tissue samples from control and CHF dogs were used for fibroblast isolation or snap-frozen and stored at −80°C for confocal imaging and real-time reverse-transcription polymerase chain reaction.

Confocal Imaging

Serial 14-μm cryosections were prepared from control and CHF (n=3 dogs each) tissues as previously described.[12] Slides were incubated with mouse anti-αSMA and goat anti-vimentin primary antibodies (both 1/200), followed by donkey anti-mouse AF555 and donkey anti-goat AF488 secondary antibodies (both 1/600), with parallel negative controls omitting primary antibodies. Slides were imaged in Z series every 0.25 μm with a Zeiss LSM-510 inverted confocal microscope. Z series images were deconvolved with Huygens Professional 3.0 software. Matched atrial and ventricular tissue analysis was performed at equal magnifications over equivalent tissue areas and thickness. αSMA-vimentin coexpression (red-green overlap) was quantified with a SigmaScan Pro v.4 (Systat Software Inc, Richmond, Calif).

TaqMan Real-Time Reverse-Transcription Polymerase Chain Reaction

Total RNA was extracted from control (n=5) and CHF (n=7) atrial and ventricular tissue samples. Real-time reverse-transcription polymerase chain reaction was performed as described previously.[9] Fluorescence signals were detected in duplicate, normalized to 18S-ribosomal RNA, and quantified with MxPro quantitative polymerase chain reaction software (Stratagene Corp, La Jolla, Calif).

Flow Cytometry

Freshly isolated control (n=4) and CHF (n=4) atrial and ventricular fibroblasts were washed 8 to 10 times in PBS, strained, and then permeabilized/fixed in cold 75% ethanol. Samples were stored at −20°C until analysis. When pelleted, cells were resuspended and incubated (4°C for 30 minutes) in staining solution containing propridium iodide at $\approx 1\times10^6$ cells per mL. Propridium-iodide fluorescence was obtained with a FACScan and CellQuest Pro software (both from BD Bioscience, Franklin Lakes, NJ).

Statistical Analysis

Data are presented as mean±SEM. Atrial versus ventricular data were analyzed by paired *t* tests in the absence of a potentially interacting factor. Otherwise, 2-way repeated-measures ANOVA was applied with models using either 1 or 2 repeated factors (for details, see the online Methods). In the case of a significant interaction between factors, contrasts based on the global model were used to compare cardiac regions (atrial or ventricular) within the other main factor (time [day 0, 1, 2, 3, and 7], group [control versus CHF], or treatment [vehicle versus AG1295]). Criteria for normal distribution of residuals were verified for all statistical models. A 2-tailed value of $P<0.05$ was considered statistically significant.

The authors had full access to and take full responsibility for the integrity of the data. All authors have read and agree to the manuscript as written.

Results

In Vitro Analyses of Atrial-Ventricular Fibroblast Differences

We first addressed differential characteristics of highly purified primary-passaged atrial versus ventricular fibroblasts, a well-established preparation for studying fibroblast properties.[9,10]

Cellular Organization and Morphology

Bright-field microscopic images of primary-passage fibroblasts are shown in Figure 1A through 1H. Cells moved from an initial rounded morphology toward a more elongated phenotype. This transition occurred faster in atrial cells (significant interaction between cell type and time: F=17.22; *df*n=4; *df*d=20; $P<0.0001$). The results of blinded quantitative analysis are shown in Figure 1I. Half-maximal growth was reached in ≈1.4 days by atrial cells compared with ≈2.2 days for ventricular ($P<0.01$) (interaction between cell type and time: F=9.20; *df*n=4; *df*d=25; $P=0.0001$). At confluence (day 7), despite similar surface areas (1.54±0.10 for atrial versus 1.61±0.08 for ventricular; P=NS), primary-passage atrial cells displayed distinct organization and morphology (Figure 2A and 2B). Atrial fibroblasts showed more long-axis alignment and elongated morphologies (Figure 2C) with greater long-axis and lesser short-axis dimensions (Figure 2D).

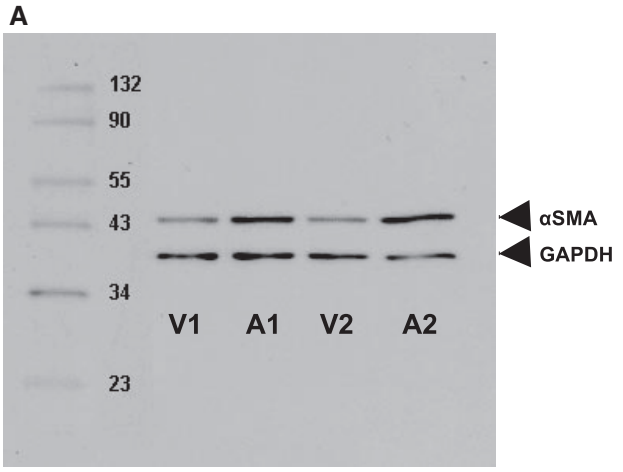

Figure 3. A, Representative αSMA (top) and GAPDH (bottom) bands from 2 ventricular (Vent) and atrial (At) pairs. Molecular mass markers are on the left. B, Mean±SEM αSMA band intensities relative to GAPDH. n=6 pairs. *$P<0.05$.

αSMA Expression

Differentiating fibroblasts acquire a highly secretory myofibroblast phenotype characterized by αSMA expression, which correlates with increased secretion of profibrotic extracellular matrix components like collagen and fibronectin.[13,14] We therefore compared αSMA expression in atrial and ventricular fibroblasts grown to confluence in 7% FBS. Figure 3A shows representative immunoblots with distinct bands corresponding to αSMA (≈42 kDa) and GAPDH (≈36 kDa). αSMA expression was significantly greater in atrial than ventricular fibroblasts (Figure 3B).

Stimulus-Induced Proliferation Responses

Both enhanced secretory activity of individual fibroblasts and fibroblast proliferation, which increases fibroblast number, can contribute to fibrosis. We therefore compared growth stimulus–induced proliferative responses of first-passage atrial and ventricular fibroblasts plated at equal density (Figure 4A through 4F). Basal [^{3}H]thymidine uptake was indistinguishable in serum-free conditions (797±83 disintegrations per minute in ventricular versus 802±105 disintegrations per minute in atrial; P=NS); however, proliferation of atrial cells was consistently greater than that of matched ventricular fibroblasts when stimulated with a range of

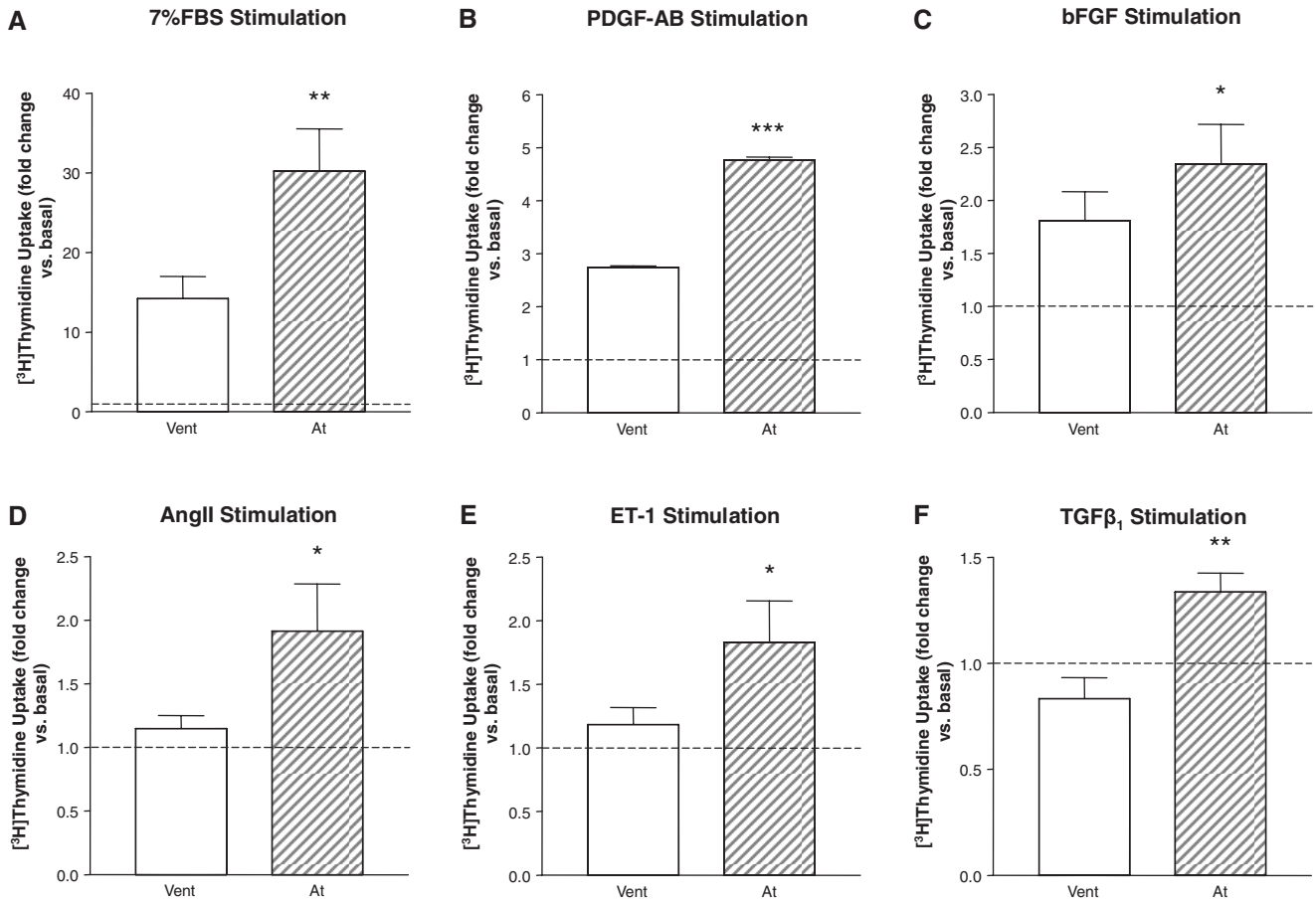

Figure 4. [^{3}H]Thymidine (mean±SEM) incorporation in first-passage atrial (At) and ventricular (Vent) fibroblasts under stimulation by 7%-FBS (A), PDGF-AB (10 ng/mL; B), basic fibroblast growth factor (bFGF; 5 ng/mL; C), angiotensin II (AngII; 100 nmol/L; D), endothelin-1 (ET-1; 10 nmol/L; E), and TGFβ_1 (0.15 ng/mL; F). Dashed horizontal line indicates baseline (nonstimulated cells); n=8 to 11 observations for each experiment. *$P<0.05$; **$P<0.01$; ***$P<0.001$, At vs Vent.

growth factors, including FBS, PDGF, basic fibroblast growth factor, angiotensin II, endothelin-1, and TGFβ_1.

Differences in Gene Expression Profile of Atrial Versus Ventricular Fibroblasts

To assess gene expression differences, we performed transcriptome-wide microarray analyses of atrial and ventricular fibroblasts grown to confluence in 7% FBS. Statistically significant differential expression was noted for 225 probe sets. Of these, 60 sequences had no homology to known proteins, leaving 165 probe sets. In some cases, multiple probe sets corresponded to the same gene. The Table shows genes with consistent differential expression on each of several probe sets (82 probe sets accounting for 34 genes). The differentially expressed genes were implicated in important processes involved in remodeling, including extracellular matrix formation (fibronectin, laminin, fibulin, collagen triple-helix repeat containing 1), cell signaling (PDGFRα, secreted frizzle-related protein, vascular endothelial growth factor, angiopoietin, insulin-like growth factor binding protein), cell structure (keratin type 1), and metabolism (xanthine dehydrogenase).

We then cross-referenced each probe set showing a significant difference against the complete microarray library from Affymetrix to identify all available probe sets corresponding to each gene. Online-only Data Supplement Table I lists each gene with at least 1 significantly changed probe set, the mean relative atrial-ventricular expression for all significantly different corresponding probe sets, and the number of probe sets showing statistically significant changes per total number of probe sets for that gene. When all probe sets showed differences in the same direction (even though some may not have been statistically significant), no asterisk is shown (Probe set divergence is indicated by an asterisk). Online-only Data Supplement Table II provides detailed data for each gene with at least 1 significantly changed probe set. For 35 single statistically significant probe sets, no additional probe sets were in the complete Affymetrix chip library. For 28 probe sets, additional probe sets showed a similar fold change trend that did not reach statistical significance. The remaining 20 single-hit probe sets had at least 1 additional probe set with directionally different pairwise fold changes that could represent false-positive detections.

Atrial Versus Ventricular Fibroblast Properties In Vivo

Having found important differences between atrial and ventricular fibroblasts in vitro, we sought evidence for differential atrial-ventricular fibroblast behaviors in intact hearts.

Table. Genes From First-Passage Atrial and Ventricular Fibroblasts (n=5 Dogs) That Were Differentially Expressed on Each of Several Probe Sets

Functional Class and Gene	Fold Change± SEM (At/Vent)	Probe Sets, n
Extracellular matrix		
Collagen triple-helix repeat containing 1	1.80±0.05	2
Fibronectin 1	3.21±0.42	5
Fibulin-1	1.91±0.07	3
Fibulin-5	4.15±0.29	3
Laminin β-1	2.86±0.41	3
Matrix Gla protein	2.73±0.26	2
Cell signaling		
Angiopoietin-like 4 protein	0.54±0.02	2
Cytoplasmic tyrosine protein kinase BMX	4.22±1.24	2
Phosphatidic acid phosphatase type 2B	1.74±0.07	3
PDGFRα	3.38±1.15	2
Regulator of G-protein signaling 2, 24 kDa	3.46±0.07	2
Serum/glucocorticoid regulated kinase	1.91±0.21	3
Vascular endothelial growth factor D	0.40±0.08	2
Metabolism		
Cysteine dioxygenase type I	5.54±2.57	4
Glycosyltransferase 8	2.26±0.11	2
Peptidylglycine α-amidating monooxygenase	1.97±0.03	2
Xanthine dehydrogenase/oxidase	2.48±0.61	2
Structural		
Keratin type I	0.46±0.03	3
Tetranectin	4.58±2.28	2
Tetraspanin 12	2.12±0.19	2
Cell cycle and differentiation		
Four-and-a-half LIM domains 1	1.95±0.13	2
Polo-like kinase 2	1.96±0.10	2
Secreted frizzle-related protein 1	27.85±15.84	2
Immunity and coagulation		
CD59 antigen p18-20	1.82.14	2
Complement component C3	3.82±1.26	2
Sushi repeat-containing protein	1.75±0.08	3
Binding protein		
Cellular retinol-binding protein	2.59±0.34	2
Insulin-like growth factor binding protein 6	2.38±0.16	2
Secreted modular calcium-binding protein 1	5.97±3.68	2
Adhesion and migration		
Dermatopontin	3.34±0.16	2
Tropomodulin 1	2.48±0.17	2
Protease and RNase/inhibitors		
Protease inhibitor 7	4.26±0.17	3
Ribonuclease 4	2.25±0.37	2
Miscellaneous		
Placenta-specific gene 8 protein (C15 protein)	5.44±2.34	3
Total=34	...	82

Myofibroblast Content

We first compared atrial and ventricular myofibroblast content with immunofluorescence labeling of αSMA (red) and vimentin (green) in control and CHF tissue sections. Representative images are shown in Figure 5A through 5D. αSMA staining and vimentin staining were observed in the interstitial regions between bundles of surrounding cardiomyocytes (unlabeled; visible in the overlaid phase-contrast images; online-only Data Supplement Figure III shows image without phase-contrast overlay), with more extensive staining and coexpression (yellow) in CHF. Both markers and their coexpression were more evident in atrial compared with ventricular tissue. Vimentin/αSMA coexpression (an index of myofibroblast content) was greater in atria than in ventricles for both control and CHF hearts, and CHF significantly increased atrial coexpression (Figure 5E). A statistically significant interaction was present between tissue type (atrium versus ventricle) and condition (control versus CHF) in determining coexpression ($F=30.89$; dfn$=1$; dfd$=4$; $P=0.0051$), indicating that tissue type is a determinant of the fibroblast response to CHF.

Mitotic Indexes in Freshly Separated Fibroblasts

We subsequently used flow cytometry to evaluate in vivo fibroblast proliferative indexes in freshly isolated control and CHF atrial and ventricular fibroblasts (Figure 5F). Online-only Data Supplement Figure IV shows examples of the dual-parameter dot plots used for gating (Figure IVA) and histogram analysis of DNA content in propridium-iodide–stained cells (Figure IVB). Cells derived from control atria and ventricles exhibited comparable numbers of dividing cells (in either cell cycle S or G2/M phase). CHF slightly increased ventricular fibroblast division rates but greatly increased atrial fibroblast division. The interaction between tissue type and condition was significant ($F=40.43$; dfn$=1$; dfd$=6$; $P=0.0007$), indicating that cardiac chamber is a determinant of the in vivo fibroblast proliferative response to CHF.

Fibroblast Secretory Gene Function

To assess in vivo fibroblast secretory gene function, control and CHF tissue samples were analyzed by real-time reverse-transcription polymerase chain reaction, choosing fibroblast-selective extracellular matrix genes *Col1*, *FN1*, and *Col3*.[1] All 3 genes were expressed at low levels in control atrial and ventricular tissues, and CHF resulted in robust atrial upregulation (Figure 6A through 6C). A significant interaction was observed between chamber and condition for each of *Col1* ($F=28.34$; dfn$=1$; dfd$=9$; $P=0.0005$), *FN1* ($F=37.29$; dfn$=1$; dfd$=10$; $P=0.0001$), and *Col3* ($F=36.11$; dfn$=1$; dfd$=9$; $P=0.0002$) mRNA expression, indicating that the fibroblast secretory gene response to CHF is chamber specific.

Potential Role of PDGF in Differential Behaviors

Both PDGF and its α receptor were significantly more strongly expressed in atrial than ventricular fibroblasts (online-only Data Supplement Table I). PDGF modulates growth factors,[15] and a tightly regulated autocrine PDGF loop is responsible for bimodal proliferation of connective tissue

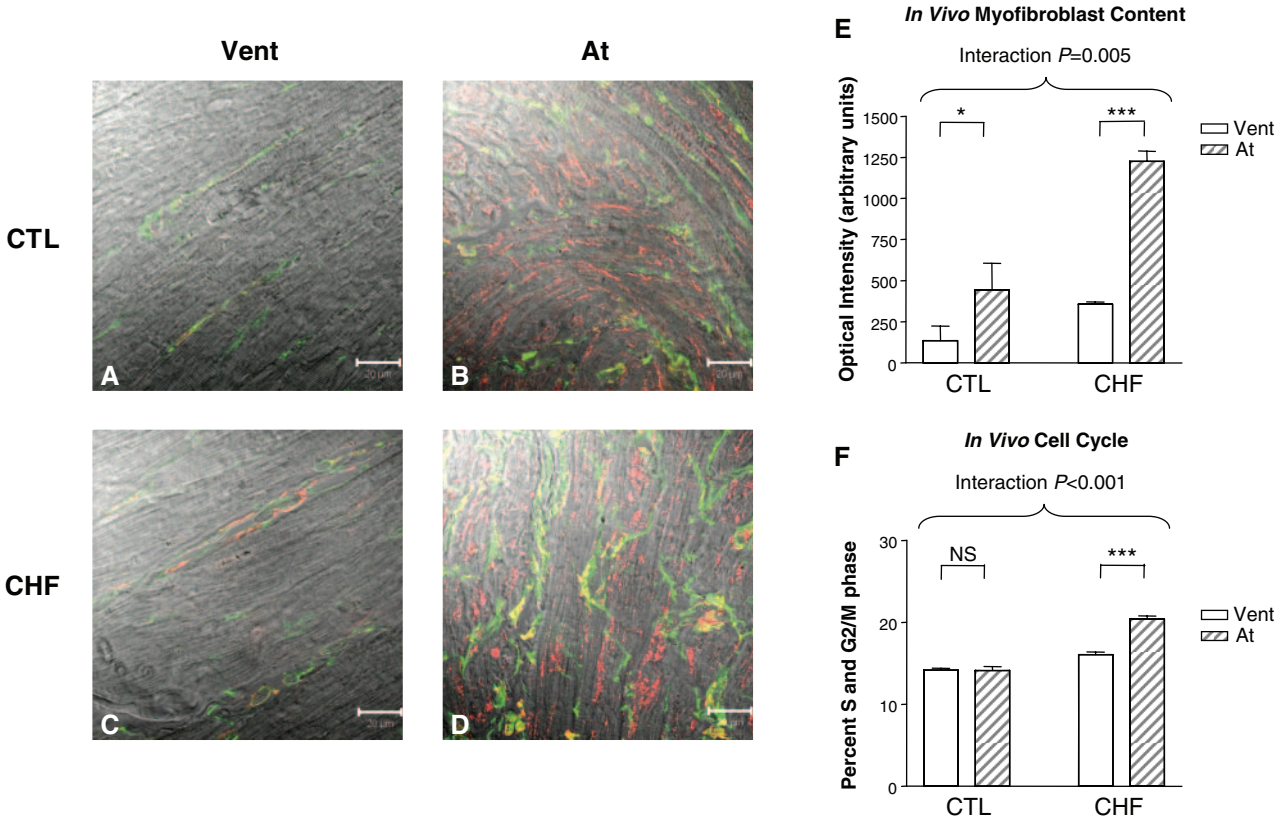

Figure 5. A through D, Immunofluorescent confocal images from 1 representative dog per group (superimposed over phase-contrast images; magnification ×63; bar=20 μm). Red indicates αSMA; green, vimentin. E, Mean±SEM myofibroblast content; n=3 control (CTL), 3 CHF dogs. F, Percentage of cells in S and G2/M phase by flow cytometry (mean±SEM); n=4 control, 4 CHF dogs. Vent indicates ventricular; At, atrial. *$P<0.05$; ***$P<0.001$.

cells in response to TGFβ1.[16] We therefore assessed the potential role of PDGF in differential atrial-ventricular fibroblast behaviors.

We first evaluated atrial-ventricular PDGF-B and PDGFRα gene expression differences in intact tissue samples corresponding to the microarray findings for cultured fibroblasts. PDGF-B expression was not significantly different in control tissues but was differentially enhanced in CHF dog atria (Figure 6D). PDGFRα expression was greater in atria than ventricles at baseline, and this difference was exaggerated by CHF (Figure 6E). A statistically significant interaction was observed between tissue origin and condition for both PDGF-B ($F=23.39$; dfn=1; dfd=9; $P=0.0009$) and PDGFRα ($F=14.58$; dfn=1; dfd=10; $P=0.0034$) expression. We next confirmed differential atrial-ventricular protein expression of PDGFRα and αSMA in isolated control and CHF fibroblasts (Figure 7). CHF further enhanced baseline atrial-ventricular differences in PDGFRα ($F=28.61$; dfn=1; dfd=10; $P=0.0003$) and αSMA ($F=18.17$; dfn=1; dfd=10; $P=0.0017$) expression, consistent with whole-tissue mRNA data and supporting a role for PDGF signaling in CHF fibroblast responses.

We then addressed the potential functional role of differential atrial-ventricular PDGFR expression by determining whether PDGF signaling is important for enhanced atrial fibroblast proliferation responses to other factors. Atrial and ventricular fibroblast [^{3}H]thymidine incorporation was compared in response to 24-hour stimulation with FBS (Figure 8A) and TGFβ1 (Figure 8B) in the presence and absence of the PDGFR tyrosine kinase antagonist AG1295 (10 μmol/L). AG1295 significantly reduced the atrial and ventricular fibroblast proliferative responses induced by FBS and eliminated the differential atrial-ventricular fibroblast behavior. Similarly, the differential response of atrial fibroblasts to TGFβ1 stimulation was eliminated by AG1295. The interactions between cell type and PDGF-inhibiting effects were highly significant ($F=54.91$; dfn=1; dfd=5; $P=0.0007$ for FBS; and $F=60.83$; dfn=1; dfd=5; $P=0.0006$ for TGFβ1). These data indicate that PDGF signaling is essential for the discrepant atrial-ventricular fibroblast responses induced by FBS and TGFβ1.

Discussion

We have demonstrated that despite overall phenotypic similarity, atrial fibroblasts are consistently more reactive than ventricular fibroblasts and show distinct growth characteristics, proliferative responses, and gene expression profiles. PDGF-related differences play an important role in atrial-ventricular fibroblast proliferative response discrepancies.

Evidence for Differential Atrial-Ventricular Fibrotic Remodeling

Cardiac chamber–specific gene expression patterns exist throughout development[17] and occur in normal[18–20] and

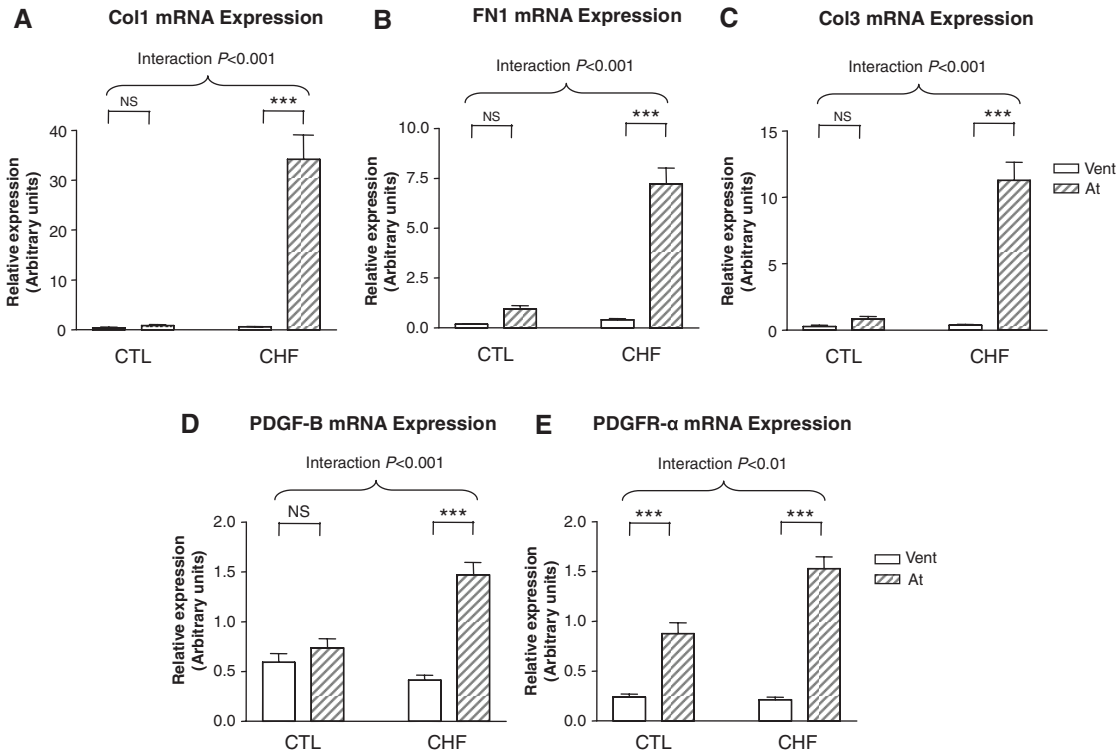

Figure 6. *Col1* (A), *FN1* (B), *Col3* (C), PDGF-B (D), and PDGFRα (E) mRNA expression in atrial (At) and ventricular (Vent) tissue samples. Values are mean±SEM. n=5 control (CTL), 7 CHF dogs. ***$P<0.001$.

diseased[21,22] myocardium. Cardiac overexpression of junctin, an integral membrane protein colocalizing with ryanodine receptors and calsequestrin, causes markedly enlarged, severely fibrotic atria with much more limited ventricular fibrosis.[23] Overexpression of the gene expression regulator cAMP response element modulator produces hypertrophic cardiomyopathy with markedly enlarged atria but not ventricles.[24] Cardiac angiotensin-converting enzyme overexpression causes atrial dilation, fibrosis, and AF despite normal ventricular function and structure.[8] Mice with constitutively active TGFβ_1 show atrial fibrosis without changes in ventricular size, function, or structure.[6,7] In all these genetically engineered mouse models, atrial fibrosis greatly exceeds ventricular fibrosis despite similar transgene expression in both regions. Some of these models (eg, angiotensin-converting enzyme and TGFβ_1 overexpression) lack CHF, excluding differential atrial-ventricular hemodynamic stress.

Relation to Previous Studies

Our finding of greater myofibroblast content in normal atria versus ventricles agrees with observations of greater fibrous tissue and extracellular matrix volume in normal atria,[25,26] previously hypothesized to be related to chamber-specific functional requirements, pressure, and volume.[27] Larger myofibroblast content in CHF atria compared with ventricles agrees with previous findings of greater fibrosis in the atria versus ventricles of CHF dogs,[5] particularly in light of data showing that increased fibroblast density correlates with myocardial fibrosis.[28]

Our observations contribute to a growing literature on tissue-specific fibroblast diversity. Rat fibroblasts cultured from skeletal muscle, dermis, and lung show different patterns of αSMA expression, cytoskeletal pattern, and cell adhesion structures.[29] Human fibroblasts cultured from proximal airways are distinct from peripheral lung parenchymal fibroblasts in size, morphology, and proliferative and secretory function.[30] Discrete fibroblast populations in rat lung tissue maintain their characteristic features from the second through fourth passages.[31] Differential responses to growth factors and gene expression patterns are seen in cultured human fibroblasts obtained from different periodontal regions.[32–34] Cultured 10th-passage human skin fibroblasts from different anatomic sites display discrete gene expression patterns, with notable differences in genes implicated in extracellular matrix synthesis, lipid metabolism, and cell signaling.[35] Our work shows that atrial and ventricular fibroblasts display many differences corresponding to previously observed variations in other tissue systems, including differences in morphology, secretory and proliferative function, response to growth factors, and gene expression. Our observations of in vivo cardiac systems and freshly isolated fibroblasts suggest that atrial-ventricular differences are particularly manifest in an important pathological condition (CHF) in which preferential atrial fibrosis is of pathophysiological relevance to a clinically important arrhythmia, AF.[4,5]

Potential Mechanisms Underlying Atrial-Ventricular Fibroblast Differences

Cardiac fibroblasts derive from mesenchymal cells that originate in the proepicardial organ and produce chamber-specific cardiac development.[36] Myocardial scar fibro-

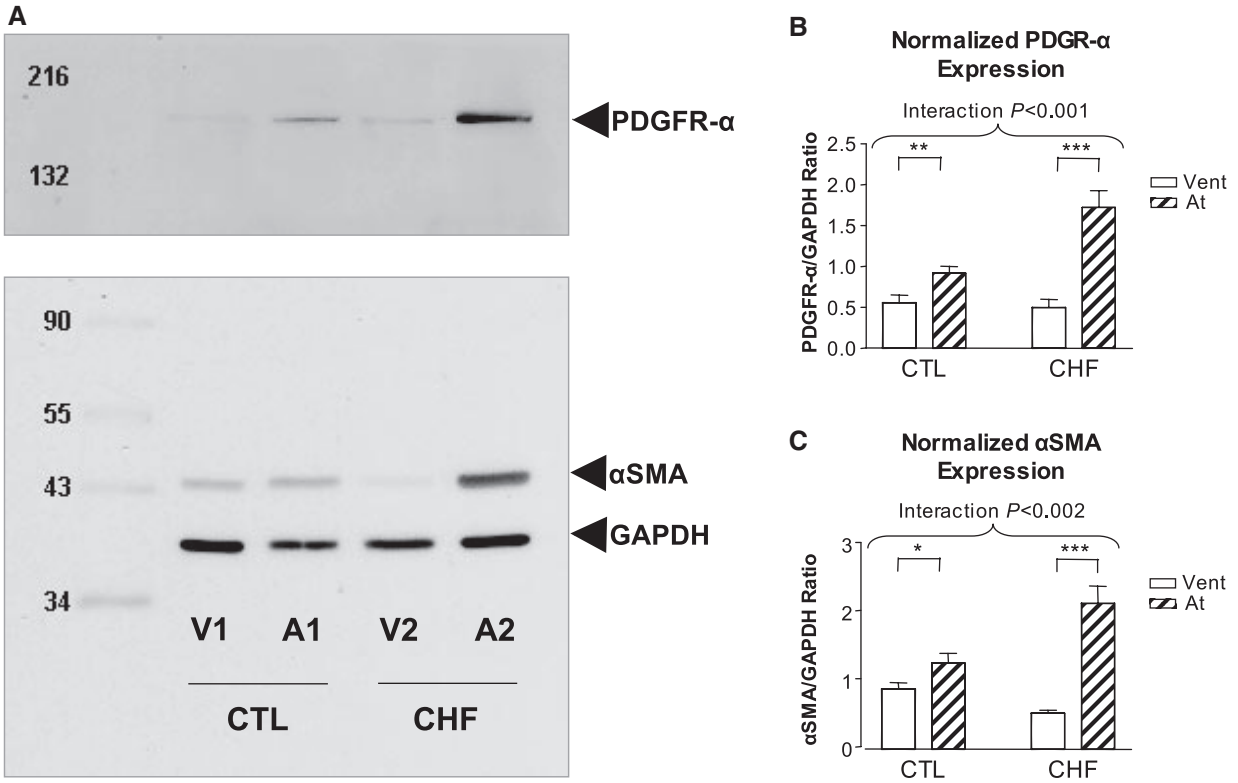

Figure 7. A, Representative corresponding PDGFRα (top), αSMA (middle), and GAPDH (bottom) bands for isolated ventricular (Vent) and atrial (At) fibroblast pairs from 1 control (CTL) and 1 CHF dog. Molecular mass markers are on the left. PDGFRα (B) and αSMA (C) band intensities relative to GAPDH. Values are mean±SEM. n=6 hearts per observation. *$P<0.05$; **$P<0.01$; ***$P<0.001$.

blasts derive predominantly from resident intracardiac fibroblast populations[37] and endothelial-to-mesenchymal transition,[38] although there also is evidence for a contribution from bone marrow–derived cells.[39] The atrial-ventricular fibroblast differences we observed may be due to intrinsic chamber-specific differences or to effects of the specific atrial hemodynamic, neurohumoral, and structural environment or their combination. We detected atrial-ventricular gene expression differences in important signaling molecules that could contribute to the functional differences we observed. PDGF appeared to play a particularly important role. PDGF, a regulatory peptide stimulated by tissue injury, activates PDGFR tyrosine kinase, initiating multiple secondary messenger signaling cascades,[15,40] and synergizes with other growth factors, in particular TGFβ_1, in an autocrine and a paracrine fashion.[16,41,42] TGFβ_1-induced proliferation in some systems requires the induction of PDGF in the presence of unmethylated PDGF DNA.[42] Cardiac-restricted overexpression of either PDGF-C or PDGF-D isoforms cause fibrosis and dilated cardiomyopathy.[43,44] PDGF is important in myofibroblast differentiation in vivo,[45,46] alters fibroblast morphology, and induces collagen synthesis[47] and proliferation[48] in vitro. The elimination of atrial-ventricular fibroblast response differences to FBS and TGFβ_1 after treatment with AG1295 suggests that a substantial part of the differential cell type–specific response is mediated by PDGF, likely because of preferential atrial expression of both PDGF and its PDGFR.

Novelty and Potential Significance

To the best of our knowledge, this is the first direct comparison of atrial and ventricular fibroblasts and the first demonstration that they show systematic differences. These differences may contribute to the selective atrial fibrosis observed in various experimental models and to AF-promoting atrial fibrosis in humans. Furthermore, our observation that PDGF plays a central role in atrial-ventricular fibroblast differences provides insights into underlying molecular mechanisms. Our results may account (at least in part) for previously enigmatic findings such as the fact that mice expressing constitutively active TGFβ_1, with comparable atrial and ventricular TGFβ_1 activation, show substantial atrial fibrosis and an AF phenotype but little or no ventricular remodeling.[6,7] Cardiac fibroblast function has been studied in detail but typically with the use of ventricular fibroblasts. Our findings indicate that caution may be needed in extrapolating the conclusions of studies performed with 1 cardiac fibroblast subtype to the other. Interventions to prevent atrial fibrosis are of potential therapeutic interest for AF.[49] PDGF and associated signaling pathways may present new opportunities for preventing arrhythmogenic atrial structural remodeling.

Potential Limitations

Because [^{3}H]thymidine incorporation assays measure only 24 hours of stimulus-induced proliferation, our results relate to short-term cellular reactivity under conditions that cannot entirely model the complex in vivo milieu. We were

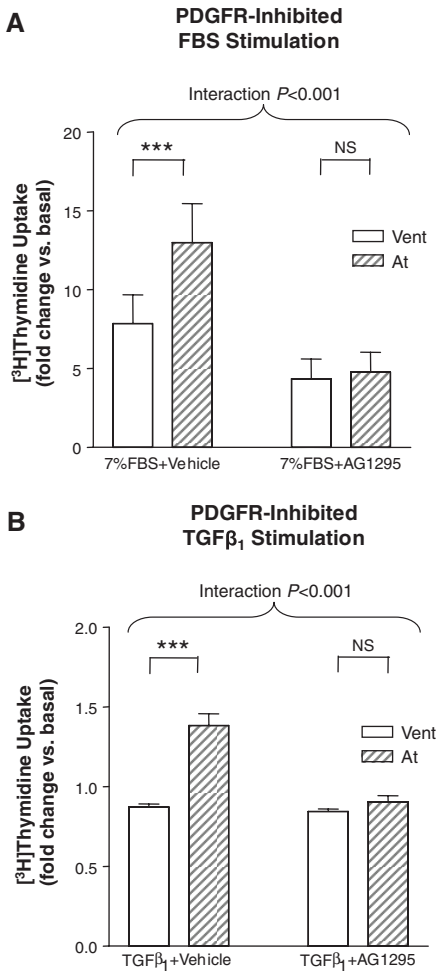

Figure 8. [^{3}H]thymidine incorporation (mean±SEM) in first-passage atrial (At) and ventricular (Vent) fibroblasts treated with 7% FBS (A) and TGFβ_1 (0.15-ng/mL; B) in the presence and absence of the PDGFR inhibitor AG1295 (10 μmol/L). n=6 per observation. ***$P<0.001$.

puzzled by the limited ventricular fibroblast responses to some stimuli, in particular the absence of proliferation enhancement with angiotensin II, given the known importance of this mediator in cardiac remodeling. On reviewing the literature, we noted that the reported fibroblast proliferative responses show significant discrepancies, possibly related to technical differences among studies, and that many investigators have failed to show angiotensin II–induced ventricular fibroblast proliferation.[50] We therefore focused our analysis on differential atrial-ventricular responses, which we found to be very consistent in our system. Gene expression analysis revealed a relatively small number of atrial-ventricular differences (225 of ≈43 000 probe sets). The statistical approach that we used (significance analysis for microarrays with q<5) implies that <5% of genes identified as differentially expressed represent false-positive detection (ie, there should be no more than ≈12 false positives among the 225 differences identified). Interestingly, the differentially expressed secreted extracellular matrix protein genes fibronectin, laminin, fibulin, and collagen triple-helix repeat containing 1 are consistently upregulated in atrial cells versus ventricular. The microarray data do not address proteomic differences like posttranscriptional/translational modifications and regulatory changes and represent only a single time point snapshot of the continually changing transcriptome. We also considered only left atrial and ventricular fibroblasts and have not evaluated right-sided cells.

Much of our work was performed in first-passage cultured cardiac fibroblasts. Most previous studies of tissue- and organ-specific fibroblast properties were performed in cultured fibroblasts from the 2nd through 10th passages[29–35] because of small cell numbers and incomplete purity in freshly isolated fibroblast samples. We cannot exclude the possibility that fibroblast properties were affected by the isolation and culture procedure. Our observations of greater numbers of myofibroblasts in atrial versus ventricular tissue samples with exaggeration in response to CHF, of greater fibroblast proliferative indexes in CHF atrium versus ventricle, and of differential atrial-ventricular expression of fibroblast-selective markers in snap-frozen tissue samples, particularly in CHF, all support the relevance of our in vitro findings to the in vivo context. We studied responses in 2-dimensional media, which may differ from behaviors in 3-dimensional matrixes. In addition, cocultures of myocytes, fibroblasts, and tissue sections were not used. Such systems might be very useful in determining interactions between the different cell types, which may reflect the in vivo situation even better.

Acknowledgments

We thank Marième Cossette, Nathalie Henley, Nathalie L'Heureux, Chantal St-Cyr, Louis Villeneuve, Ling Xiao, and Yung-Hsin Yeh for technical assistance and suggestions and France Thériault for secretarial support.

Sources of Funding

This work was supported by the Canadian Institutes of Health Research (CIHR) and the Quebec Heart and Stroke Foundation. B. Burstein received a CIHR MD/PhD studentship. Dr Calderone is a Chercheur-boursier National of the Fonds de la recherche en santé du Québec.

Disclosures

None.

References

1. Cleutjens JP, Verluyten MJ, Smiths JF, Daemen MJ. Collagen remodeling after myocardial infarction in the rat heart. *Am J Pathol*. 1995;147:325–338.
2. Dorian P. The future of atrial fibrillation therapy. *J Cardiovasc Electrophysiol*. 2006;17(suppl 2):S11–S16.
3. Nattel S, Opie LH. Controversies in atrial fibrillation. *Lancet*. 2006;367:262–272.
4. Li D, Fareh S, Leung TK, Nattel S. Promotion of atrial fibrillation by heart failure in dogs: atrial remodeling of a different sort. *Circulation*. 1999;100:87–95.
5. Hanna N, Cardin S, Leung TK, Nattel S. Differences in atrial versus ventricular remodeling in dogs with ventricular tachypacing-induced congestive heart failure. *Cardiovasc Res*. 2004;63:236–244.
6. Nakajima H, Nakajima HO, Salcher O, Dittie AS, Dembowsky K, Jing S, Field LJ. Atrial but not ventricular fibrosis in mice expressing a mutant

transforming growth factor-beta(1) transgene in the heart. *Circ Res*. 2000;86:571–579.
7. Verheule S, Sato T, Everett T, Engle SK, Otten D, Rubart-von der LM, Nakajima HO, Nakajima H, Field LJ, Olgin JE. Increased vulnerability to atrial fibrillation in transgenic mice with selective atrial fibrosis caused by overexpression of TGF-beta1. *Circ Res*. 2004;94:1458–1465.
8. Xiao HD, Fuchs S, Campbell DJ, Lewis W, Dudley SC Jr, Kasi VS, Hoit BD, Keshelava G, Zhao H, Capecchi MR, Bernstein KE. Mice with cardiac-restricted angiotensin-converting enzyme (ACE) have atrial enlargement, cardiac arrhythmia, and sudden death. *Am J Pathol*. 2004;165:1019–1032.
9. Burstein B, Qi X, Yeh YH, Calderone A, Nattel S. Atrial cardiomyocyte tachycardia alters cardiac fibroblast function: a novel consideration in atrial remodeling. *Cardiovasc Res*. 2007;76:442–452.
10. Drapeau J, El Helou V, Clement R, Bel-Hadj S, Gosselin H, Trudeau LE, Villeneuve L, Calderone A. Nestin-expressing neural stem cells identified in the scar following myocardial infarction. *J Cell Physiol*. 2005;204:51–62.
11. Cardin S, Libby E, Pelletier P, Le Bouter S, Shiroshita-Takeshita A, Le Meur N, Leger J, Demolombe S, Ponton A, Glass L, Nattel S. Contrasting gene expression profiles in two canine models of atrial fibrillation. *Circ Res*. 2007;100:425–433.
12. Melnyk P, Ehrlich JR, Pourrier M, Villeneuve L, Cha TJ, Nattel S. Comparison of ion channel distribution and expression in cardiomyocytes of canine pulmonary veins versus left atrium. *Cardiovasc Res*. 2005;65:104–116.
13. Gabbiani G. Evolution and clinical implications of the myofibroblast concept. *Cardiovasc Res*. 1998;38:545–548.
14. Petrov VV, Fagard RH, Lijnen PJ. Stimulation of collagen production by transforming growth factor-beta1 during differentiation of cardiac fibroblasts to myofibroblasts. *Hypertension*. 2002;39:258–263.
15. Waltenberger J. Modulation of growth factor action: implications for the treatment of cardiovascular diseases. *Circulation*. 1997;96:4083–4094.
16. Battegay EJ, Raines EW, Seifert RA, Bowen-Pope DF, Ross R. TGF-beta induces bimodal proliferation of connective tissue cells via complex control of an autocrine PDGF loop. *Cell*. 1990;63:515–524.
17. Franco D, Lamers WH, Moorman AF. Patterns of expression in the developing myocardium: towards a morphologically integrated transcriptional model. *Cardiovasc Res*. 1998;38:25–53.
18. Tabibiazar R, Wagner RA, Liao A, Quertermous T. Transcriptional profiling of the heart reveals chamber-specific gene expression patterns. *Circ Res*. 2003;93:1193–1201.
19. Barth AS, Merk S, Arnoldi E, Zwermann L, Kloos P, Gebauer M, Steinmeyer K, Bleich M, Kaab S, Pfeufer A, Uberfuhr P, Dugas M, Steinbeck G, Nabauer M. Functional profiling of human atrial and ventricular gene expression. *Pflugers Arch*. 2005;450:201–208.
20. Ellinghaus P, Scheubel RJ, Dobrev D, Ravens U, Holtz J, Huetter J, Nielsch U, Morawietz H. Comparing the global mRNA expression profile of human atrial and ventricular myocardium with high-density oligonucleotide arrays. *J Thorac Cardiovasc Surg*. 2005;129:1383–1390.
21. Gao Z, Xu H, DiSilvestre D, Halperin VL, Tunin R, Tian Y, Yu W, Winslow RL, Tomaselli GF. Transcriptomic profiling of the canine tachycardia-induced heart failure model: global comparison to human and murine heart failure. *J Mol Cell Cardiol*. 2006;40:76–86.
22. Kaab S, Barth AS, Margerie D, Dugas M, Gebauer M, Zwermann L, Merk S, Pfeufer A, Steinmeyer K, Bleich M, Kreuzer E, Steinbeck G, Nabauer M. Global gene expression in human myocardium-oligonucleotide microarray analysis of regional diversity and transcriptional regulation in heart failure. *J Mol Med*. 2004;82:308–316.
23. Hong CS, Cho MC, Kwak YG, Song CH, Lee YH, Lim JS, Kwon YK, Chae SW, Kim DH. Cardiac remodeling and atrial fibrillation in transgenic mice overexpressing junctin. *FASEB J*. 2002;16:1310–1312.
24. Muller FU, Lewin G, Baba HA, Boknik P, Fabritz L, Kirchhefer U, Kirchhof P, Loser K, Matus M, Neumann J, Riemann B, Schmitz W. Heart-directed expression of a human cardiac isoform of cAMP-response element modulator in transgenic mice. *J Biol Chem*. 2005;280:6906–6914.
25. Popescu LM, Gherghiceanu M, Hinescu ME, Cretoiu D, Ceafalan L, Regalia T, Popescu AC, Ardeleanu C, Mandache E. Insights into the interstitium of ventricular myocardium: interstitial Cajal-like cells (ICLC). *J Cell Mol Med*. 2006;10:429–458.
26. Hinescu ME, Gherghiceanu M, Mandache E, Ciontea SM, Popescu LM. Interstitial Cajal-like cells (ICLC) in atrial myocardium: ultrastructural and immunohistochemical characterization. *J Cell Mol Med*. 2006;10:243–257.
27. Borg TK, Sullivan T, Ivy J. Functional arrangement of connective tissue in striated muscle with emphasis on cardiac muscle. *Scan Electron Microsc*. 1982;pt4:1775–1784.
28. Bing OH, Ngo HQ, Humphries DE, Robinson KG, Lucey EC, Carver W, Brooks WW, Conrad CH, Hayes JA, Goldstein RH. Localization of alpha1(I) collagen mRNA in myocardium from the spontaneously hypertensive rat during the transition from compensated hypertrophy to failure. *J Mol Cell Cardiol*. 1997;29:2335–2344.
29. Dugina V, Alexandrova A, Chaponnier C, Vasiliev J, Gabbiani G. Rat fibroblasts cultured from various organs exhibit differences in alpha-smooth muscle actin expression, cytoskeletal pattern, and adhesive structure organization. *Exp Cell Res*. 1998;238:481–490.
30. Kotaru C, Schoonover KJ, Trudeau JB, Huynh ML, Zhou X, Hu H, Wenzel SE. Regional fibroblast heterogeneity in the lung: implications for remodeling. *Am J Respir Crit Care Med*. 2006;173:1208–1215.
31. Breen E, Falco VM, Absher M, Cutroneo KR. Subpopulations of rat lung fibroblasts with different amounts of type I and type III collagen mRNAs. *J Biol Chem*. 1990;265:6286–6290.
32. Haase HR, Clarkson RW, Waters MJ, Bartold PM. Growth factor modulation of mitogenic responses and proteoglycan synthesis by human periodontal fibroblasts. *J Cell Physiol*. 1998;174:353–361.
33. Dennison DK, Vallone DR, Pinero GJ, Rittman B, Caffesse RG. Differential effect of TGF-beta 1 and PDGF on proliferation of periodontal ligament cells and gingival fibroblasts. *J Periodontol*. 1994;65:641–648.
34. Han X, Amar S. Identification of genes differentially expressed in cultured human periodontal ligament fibroblasts vs. human gingival fibroblasts by DNA microarray analysis. *J Dent Res*. 2002;81:399–405.
35. Chang HY, Chi JT, Dudoit S, Bondre C, van de RM, Botstein D, Brown PO. Diversity, topographic differentiation, and positional memory in human fibroblasts. *Proc Natl Acad Sci U S A*. 2002;99:12877–12882.
36. Moorman AF, Christoffels VM. Cardiac chamber formation: development, genes, and evolution. *Physiol Rev*. 2003;83:1223–1267.
37. Yano T, Miura T, Ikeda Y, Matsuda E, Saito K, Miki T, Kobayashi H, Nishino Y, Ohtani S, Shimamoto K. Intracardiac fibroblasts, but not bone marrow derived cells, are the origin of myofibroblasts in myocardial infarct repair. *Cardiovasc Pathol*. 2005;14:241–246.
38. Zeisberg EM, Tarnavski O, Zeisberg M, Dorfman AL, McMullen JR, Gustafsson E, Chandraker A, Yuan X, Pu WT, Roberts AB, Neilson EG, Sayegh MH, Izumo S, Kalluri R. Endothelial-to-mesenchymal transition contributes to cardiac fibrosis. *Nat Med*. 2007;8:952–961.
39. Mollmann H, Nef HM, Kostin S, von Kalle C, Pilz I, Weber M, Schaper J, Hamm CW, Elsasser A. Bone marrow-derived cells contribute to infarct remodelling. *Cardiovasc Res*. 2006;71:661–671.
40. Booz GW, Baker KM. Molecular signalling mechanisms controlling growth and function of cardiac fibroblasts. *Cardiovasc Res*. 1995;30:537–543.
41. Chen CN, Li YS, Yeh YT, Lee PL, Usami S, Chien S, Chiu JJ. Synergistic roles of platelet-derived growth factor-BB and interleukin-1beta in phenotypic modulation of human aortic smooth muscle cells. *Proc Natl Acad Sci U S A*. 2006;103:2665–2670.
42. Simm A, Diez C. Density dependent expression of PDGF-A modulates the angiotensin II dependent proliferation of rat cardiac fibroblasts. *Basic Res Cardiol*. 1999;94:464–471.
43. Ponten A, Li X, Thoren P, Aase K, Sjoblom T, Ostman A, Eriksson U. Transgenic overexpression of platelet-derived growth factor-C in the mouse heart induces cardiac fibrosis, hypertrophy, and dilated cardiomyopathy. *Am J Pathol*. 2003;163:673–682.
44. Ponten A, Folestad EB, Pietras K, Eriksson U. Platelet-derived growth factor D induces cardiac fibrosis and proliferation of vascular smooth muscle cells in heart-specific transgenic mice. *Circ Res*. 2005;97:1036–1045.
45. Bostrom H, Willetts K, Pekny M, Leveen P, Lindahl P, Hedstrand H, Pekna M, Hellstrom M, Gebre-Medhin S, Schalling M, Nilsson M, Kurland S, Tornell J, Heath JK, Betsholtz C. PDGF-A signaling is a critical event in lung alveolar myofibroblast development and alveogenesis. *Cell*. 1996;85:863–873.
46. Lindahl P, Betsholtz C. Not all myofibroblasts are alike: revisiting the role of PDGF-A and PDGF-B using PDGF-targeted mice. *Curr Opin Nephrol Hypertens*. 1998;7:21–26.
47. Ivarsson M, McWhirter A, Borg TK, Rubin K. Type I collagen synthesis in cultured human fibroblasts: regulation by cell spreading, platelet-

derived growth factor and interactions with collagen fibers. *Matrix Biol*. 1998;16:409–425.
48. Simm A, Nestler M, Hoppe V. Mitogenic effect of PDGF-AA on cardiac fibroblasts. *Basic Res Cardiol*. 1998;93(suppl 3):40–43.
49. Nattel S, Carlsson L. Innovative approaches to anti-arrhythmic drug therapy. *Nat Rev Drug Discov*. 2006;5:1034–1049.
50. Bouzegrhane F, Thibault G. Is angiotensin II a proliferative factor of cardiac fibroblasts? *Cardiovasc Res*. 2002;53:304–312.

CLINICAL PERSPECTIVE

Cardiac tissue fibrosis is important in the progression of heart disease and plays an important role in cardiac arrhythmogenesis, particularly for atrial fibrillation. In a variety of cardiac disease models, atrial fibrosis is much more prominent than fibrosis in the ventricles, even when the profibrotic stimulus appears to be operating comparably at both the atrial and ventricular levels. This study examined the hypothesis that differences between atrial and ventricular fibroblast properties contribute to the predominant atrial fibrotic phenotype. To assess this possibility, we compared morphological, secretory, and proliferative responses of canine atrial versus ventricular fibroblasts. Atrial fibroblasts showed in vitro and in vivo behaviors indicating a greater tendency to activated myofibroblast dedifferentiation. Atrial fibroblast proliferation responses were consistently greater than ventricular responses for a variety of growth factors, including fetal bovine serum, platelet-derived growth factor, basic fibroblast growth factor, angiotensin II, endothelin-1, and transforming growth factor-β_1. Atrial tissue showed larger myofibroblast density than ventricular tissue, particularly in the presence of congestive heart failure. Congestive heart failure atria had more active fibroblast division rates and enhanced gene expression of fibroblast-selective markers compared with ventricles. Gene microarrays revealed 225 differentially expressed transcript probe sets between paired atrial and ventricular fibroblast samples, including extracellular matrix, cell signaling, and metabolism genes, and identified platelet-derived growth factor as a potential contributor to atrial-ventricular fibroblast differences. Platelet-derived growth factor inhibition eliminated atrial-ventricular fibroblast proliferative response differences. Our results suggest that important differences exist in properties of atrial versus ventricular fibroblasts, that these differences contribute to atrium-selective fibrosis, and that platelet-derived growth factor signaling may be an interesting therapeutic target for the prevention of arrhythmogenic atrial structural remodeling.